Journal of
Synchrotron
Radiation

ISSN 0909-0495

Received 21 September 2011
Accepted 30 January 2012

Quantitative performance measurements of bent crystal Laue analyzers for X-ray fluorescence spectroscopy

C. Karanfil,[a]* G. Bunker,[b,c] M. Newville,[d] C. U. Segre[b] and D. Chapman[e]

[a]Department of Physics, Faculty of Science, University of Muğla, Kötekli-Muğla 48187, Turkey, [b]Center for Synchrotron Radiation Research and Instrumentation and Department of Physics, Illinois Institute of Technology, Chicago, IL 60616, USA, [c]Quercus X-ray Technologies, LLC, Oak Park, IL 60304, USA, [d]Consortium for Advanced Radiation Sources, University of Chicago, Chicago, IL 60637, USA, and [e]Department of Anatomy and Cell Biology, University of Saskatchewan, 107 Wiggins Road, Saskatoon, SK, Canada S7N 5E5. E-mail: karanfil@mu.edu.tr

Third-generation synchrotron radiation sources pose difficult challenges for energy-dispersive detectors for XAFS because of their count rate limitations. One solution to this problem is the bent crystal Laue analyzer (BCLA), which removes most of the undesired scatter and fluorescence before it reaches the detector, effectively eliminating detector saturation due to background. In this paper experimental measurements of BCLA performance in conjunction with a 13-element germanium detector, and a quantitative analysis of the signal-to-noise improvement of BCLAs are presented. The performance of BCLAs are compared with filters and slits.

Keywords: X-ray optics; X-ray fluorescence; X-ray spectroscopy; XAFS; bent crystal analyzer; X-ray filters.

1. Introduction

X-ray fluorescence spectroscopy is an important tool for many fields of science. Its applicability to real-world samples makes it particularly well suited for *in situ* studies of advanced materials, environmental speciation and biology. Studies of dilute species require intense X-ray beams. Scattered background and fluorescence radiation present severe challenges to standard multi-element energy-dispersive detectors because of their limited count rates. For this reason a simple and practical fluorescence analyzer that eliminates most of the background before it reaches the detector was developed. Following initial exploratory measurements (Bunker & Chapman, 1995), Zhong *et al.* (1999) reported a theoretical analysis of the behavior of bent Laue optics for the bent crystal Laue analyzer (BCLA) concept. Karanfil *et al.* (2000, 2002) presented the first XAFS spectra recorded with a BCLA. Kropf *et al.* (2003, 2005) applied a different implementation of the BCLA concept to actinide materials. Kujala *et al.* (2011) published measurements made with a high-resolution implementation of the BCLA concept. Takahashi *et al.* (2006) measured XANES of geological samples using BCLAs.

These analyzers typically require beams that are limited in size to approximately 100 µm in one direction (usually vertical) and a millimeter or so in the other direction. Thus, focusing optics on the beamline are beneficial, though not absolutely required. This property makes BCLA a particularly good match for the characteristics of third-generation synchrotron sources, and the small energy bandwidth makes it a uniquely suitable choice for microfocusing beamlines (Barrea *et al.*, 2010).

Here we measure the BCLA performance and use it to estimate the improvement to be gained for various background-to-signal ratios. Experimental measurements of BCLA performance in conjunction with a 13-element germanium detector, and a quantitative analysis of the signal-to-noise improvement of BCLAs are presented.

'$Z-1$' filters combined with appropriate slits are often useful in XAFS to reduce the amount of scattered X-rays that enter the detector. Stern and Heald devised (Stern & Heald, 1979; Koningsberger & Prins, 1988) this combination with a large-area ionization chamber for dilute XAFS studies, a commercial version of which is available as a 'Lytle detector' from the EXAFS Company (http://www.exafsco.com/).

In this paper we also compare the performance of BCLAs and $Z-1$ filters and slits for the rejection of undesired background in X-ray fluorescence and XAFS measurements. In such experiments most of the background consists of elastically scattered photons at the energy of the incident X-ray beam, which is of a higher energy than the fluorescence line of interest. For an element of atomic number Z, often the element of atomic number $Z-1$ has an absorption edge that lies between the fluorescence line of interest and the elastic scatter peak. If a filter made of this element is placed between the sample and the detector, it will absorb the scattered radiation more than the fluorescence. The consequent reduc-

tion in background improves the signal-to-noise ratio. The filter itself fluoresces, producing its own background, but that can be reduced by using Soller slits that transmit the fluorescence emerging from the sample but block much of the fluorescence emerging from the filter.

This works well when the background is at a higher energy than the desired fluorescence, but when the source of background is at a lower energy than the fluorescence this approach is useless. This situation occurs when the element of interest is contained in a sample composed of elements that have a slightly lower atomic number, as is often the case in environmental and materials research. The basic problem is that $Z-1$ filters provide a low-pass filter, while what is needed in this case is a high-pass filter or, even better, a bandpass filter like the BCLA.

2. BCLA design and set-up

A thin silicon crystal is bent to a specific logarithmic spiral shape (de Broglie & Lindemann, 1914; Sakayanagi, 1982) and positioned so that it diffracts the desired X-rays at every point along its mid-line, and also a finite region to each side of the mid-line. The Laue geometry is used in which the X-rays propagate through the crystal (this affords the optic good collection efficiency). In polar coordinates (r, θ) the correct logarithmic spiral shape is given by

$$r = \rho_0 \cos(\chi - \theta_B) \exp\left[\tan(\chi - \theta_B)\,\theta\right], \quad (1)$$

where ρ_0 is the bend radius at the center of the crystal $\theta = 0$, θ_B is the Bragg angle, and χ is the crystal asymmetry angle.

The reflectivity width (Erola *et al.*, 1990) for a ray striking the bent Laue crystal with a thickness T, bending radius ρ, asymmetry angle χ, Bragg angle (energy) θ_B and Poisson ratio ν is given by

$$\Delta\theta = \frac{T}{\rho}\Big[\tan(\chi \mp \theta_B) + \frac{1}{2}(1+\nu)\sin 2\chi \pm \tan\theta_B\left(\cos^2\chi - \nu\sin^2\chi\right)\Big]. \quad (2)$$

The energy resolution of a BCLA is calculated by the differential form of the Bragg equation as

$$\frac{\Delta E}{E} = \frac{\Delta\lambda}{\lambda} = \Delta\theta\,\cot\theta_B. \quad (3)$$

The diffracted rays are deflected by twice the Bragg angle. They pass through slits that are aligned parallel to the diffracted beams, so they are not blocked. The undesired background is not diffracted, so it passes through the crystal and is blocked by the slits. An X–Y stage is used to align the system; a rotation stage is not required (Kujala *et al.*, 2011). Sufficient width is allowed for the transverse opening of the beam. The window size in the frame is defined by this width and the length of crystal that can be obtained (usually $\sim$10 cm). The crystal is attached by taping the ends to the logarithmic spiral surface of the frame over the window. Since the bender frame is asymmetric (cannot be flipped and has the same shape), the crystal must be put on the frame in the correct orientation to ensure diffraction from the desired planes [usually the (1,1,1)-type planes]. The slit holders are also designed to match the diffracted beam paths. Mounting holes are added along with holes to attach slit holders to the sides. The bent Laue analyzer is designed so that the analyzer can be easily placed at the correct position relative to the fluorescence source (the beam spot on the sample) (Fig. 1*a*).

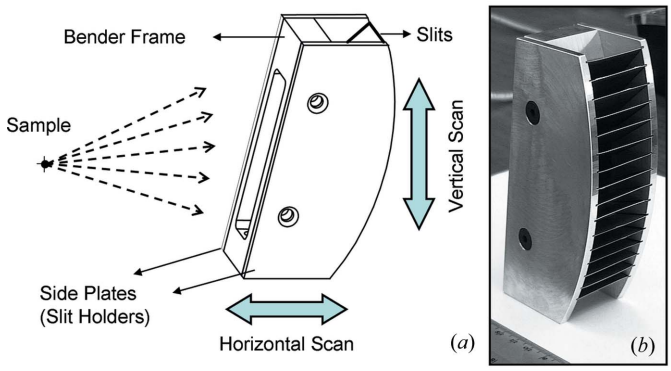

Figure 1
(*a*) Arrows indicate a vertical and a horizontal scan on the X–Y stage to find the optimum analyzer position (the narrowest rocking curve peaks). (*b*) Photograph of the back view of a bent Laue analyzer optimized for As K_α fluorescence. The material of the pure metal slits (molybdenum) was chosen to minimize slit fluorescence.

3. Measurements with germanium solid-state detector

We report here a measurement of the performance on the GSE-CARS microfocus beamline ID-13 at the Advanced Photon Source. The sample was a physical mixture of approximately 2% powdered As_2O_3 on powdered Fe_2O_3. Platinum-coated horizontal and vertical mirrors in the Kirkpatrick–Baez configuration (Kirkpatrick & Baez, 1948) were used to focus the X-ray beam down to a spot size of 5 µm × 5 µm, and to reject the harmonics. The standard configuration of the beamline uses a 13-element germanium detector, which was used in conjunction with the Laue analyzer. To avoid saturation of the detector, a $\sim$1 mm-thick polyethylene attenuator was placed in front of the Ge detector. Because of the difference in energy of the iron and arsenic fluorescence, this attenuator alone significantly reduced the proportion of Fe fluorescence.

In order for the Bragg condition to be satisfied over the surface of the crystal, a 75 µm-thick silicon wafer (2.5 cm × 9.0 cm) was bent to a logarithmic spiral shape by constraining the crystal (with 105 mm bending radius at the center, $\theta = 0^\circ$) to the surface of an aluminium form numerically machined (CNC) to the correct shape. A photograph of the analyzer is shown in Fig. 1(*b*). The crystal covers a solid angle of about 0.11 sr of the sample (As-K_α = 10.543 keV) fluorescence. The asymmetric [1,1,1] reflection of a silicon crystal was used, resulting in a 19.47° asymmetry angle. High-purity molybdenum foils (about 2.3 cm long and 0.25 mm thick) were chosen to block the direct beam but to allow the diffracted beam to pass through unattenuated. Their K absorption edge ($\sim$20 keV) cannot be excited near the energy of interest, and

Table 1
Ge detector counts of As_2O_3 in Fe_2O_3 solid solution taken with BCLA; with and without slits (integration time: 2 min).

	Germanium detector counts taken with BCLA	
	Without slits	With slits
Background (N_B)	6.51×10^6	1.62×10^5
Signal (N_S)	9.89×10^6	4.34×10^6
Effective counts (N_{eff})	5.96×10^6	4.18×10^6

their L-edge fluorescence is low enough in energy that they would be automatically filtered out by windows. The slits were spaced about 0.6 cm apart from each other (spaced at 3° intervals).

To optimize the analyzer position relative to the sample, rapid two-dimensional scans of the analyzer's horizontal and vertical positions were made. The maximum throughput of the K_α fluorescence was obtained at the same position as the best resolved peaks, indicating that there were no significant form errors in the analyzer crystal. Fig. 2 provides a quantitative measure of the extent of the background reduction, and the extent of the signal reduction by the analyzer, with a point-focused X-ray beam. The dashed line shows measurements performed with the Soller slits in place, and the solid line shows the spectrum with the Soller slits removed (with the crystal). In the first case the detected signal is composed of the diffracted beam. In the second case the signal is composed of diffracted beam, undiffracted beam and background. The multi-channel analyzer spectrum allows us to identify the count rate of each, as shown in Table 1.

4. Discussion

4.1. Analysis of the signal-to-noise improvement of BCLAs

The major source of noise in most fluorescence XAFS experiments is the statistical variation in the number of detected photons, which includes both the desired fluorescence photons (signal, N_S) and the scattered background photons (background, N_B). Since photon-counting noise scales as the square root of the total photons, $(N_S + N_B)^{1/2}$, the signal-to-noise ratio is $N_S/(N_S + N_B)^{1/2}$. It is useful to designate the square of the signal-to-noise ratio as the 'number of effective counts' (see, for example, Koningsberger & Prins, 1988; Bunker, 2010), N_{eff},

$$N_{eff} = \frac{N_S^2}{N_S + N_B} = \frac{N_S}{1 + N_B/N_S}. \quad (4)$$

The data from Table 1 indicate that inserting the slits into the analyzer reduced the iron background by a factor of 40 (with better shielding the reduction can be greater). On the other hand, the signal reduced by a factor of 2.3, indicating that about 43% of the signal was diffracted without considering the absorption of the silicon crystal. For dilute samples the benefit of reducing the background greatly outweighs the disadvantage of losing signal counts.

This can be quantitatively analyzed in terms of effective counts. Define N_S and N_B as the signal and background counts that are observed without the analyzer. If the analyzer is used, the signal counts (crystal/slits) are reduced by the reduction factor r_S, and the background counts are reduced by the factor r_B, where r_S and r_B are between 0 and 1. In this case the effective counts (in the presence of the analyzer) becomes

$$N_{eff} = r_S N_S \Big/ 1 + \frac{r_B N_B}{r_S N_S}. \quad (5)$$

By denoting the background-to-signal ratio as $A = N_B/N_S$, the ratio of the effective counts to the signal counts (which is a measure of the 'efficiency') can be expressed as

$$\frac{N_{eff}}{N_S} = \frac{r_S}{1 + (r_B/r_S)\,A}. \quad (6)$$

Experimental measurements with and without slits indicated a 40-fold background reduction and signal reduction factor of 2.3. This test was carried out because it was the most reliable way to collect precisely the same area with the same proportion of scattered light in both cases (the scattered background is not isotropic). The effect of the crystal absorption is calculated from the known absorption coefficient of silicon. The crystal thickness was 75 µm, and the absorption lengths of silicon at the Fe K_α, Fe K_β and As K_α lines are 34.03, 44.97 and 145.8 µm, respectively. Accounting for the X-ray absorption of the crystal, the reduction factors (with/without the analyzer) are $r_B = 0.003$ and $r_S = 0.26$; that is, the analyzer (crystal plus slits) caused a fourfold reduction of signal but a 330-fold reduction of background. Here, $r_S = 0.26$ also infers that, when considering the absorption of the crystal, the efficiency of the analyzer is 26%. This shows very good agreement with the theoretical calculated nominal reflectivity using the *REFLECT* computer program, 31% (Etelaniemi *et al.*, 1989).

The efficiency, which we define as the ratio of the effective counts to the raw signal counts, is plotted in Fig. 3 as a function of A. Values of A of the order of 100 are typical for systems that are dilute or have matrices that contribute a large fluor-

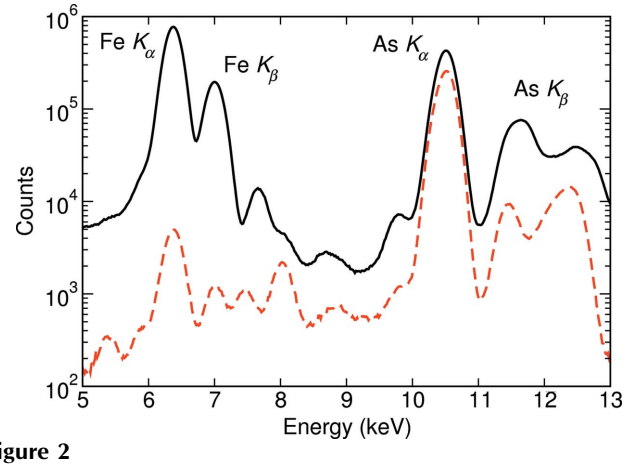

Figure 2
Multi-channel analyzer spectrum of arsenic oxide (As_2O_3) in iron oxide (Fe_2O_3) solid solution taken in 2 min. The dashed line shows measurements performed with the Soller slits in place, and the solid line shows the spectrum with the Soller slits removed (with the crystal). The analyzer effectively removes the Fe fluorescence.

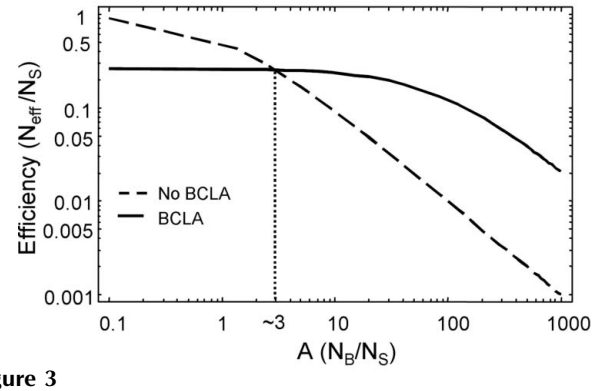

Figure 3
The efficiency ($N_{\rm eff}/N_{\rm S}$) as a function of background-to-signal ratio ($A = N_{\rm B}/N_{\rm S}$). The solid line shows the case when no BCLA is used, and the dashed line shows the improvement when using the BCLA for dilute systems $N_{\rm B}/N_{\rm S} \gg 1$.

escence background. This figure compares the effective counts as a function of A with the analyzer, and without it.

The effective counts are a function of A, $r_{\rm S}$ and $r_{\rm B}$: $N_{\rm eff}(A, r_{\rm S}, r_{\rm B})$. When the background-to-signal ratio A (in the absence of the analyzer) is greater than a specific value, the effective counts will be improved by using the Laue analyzer. The crossover point A' [obtained by setting $N_{\rm eff}(A, r_{\rm S}, r_{\rm B}) = N_{\rm eff}(A, 1, 1)$] is easily solved for $A' = (1 - r_{\rm S})/(r_{\rm S} - r_{\rm B}/r_{\rm S})$. For the case $r_{\rm S} = 0.26$, $r_{\rm B} = 0.003$, this gives $A' \cong 3.0$. At zero background ($A = 0$), the effective counts will be better without the Laue analyzer, because the analyzer does attenuate the signal counts by the ratio $r_{\rm S}$.

The improvement factor (IF) given by equation (7) is a measure of the improvement in the effective counts obtained through the use of BCLA,

$$\mathrm{IF} = \frac{r_{\rm S}\big/[1 + (r_{\rm B}/r_{\rm S})\,A]}{1/(1 + A)} = \frac{r_{\rm S}\,(1 + A)}{1 + (r_{\rm B}/r_{\rm S})\,A}. \qquad (7)$$

A log–log plot of this is shown in Fig. 4. Typical situations encountered in practice would put A between 10 and 100, corresponding to improvement factors of greater than fivefold.

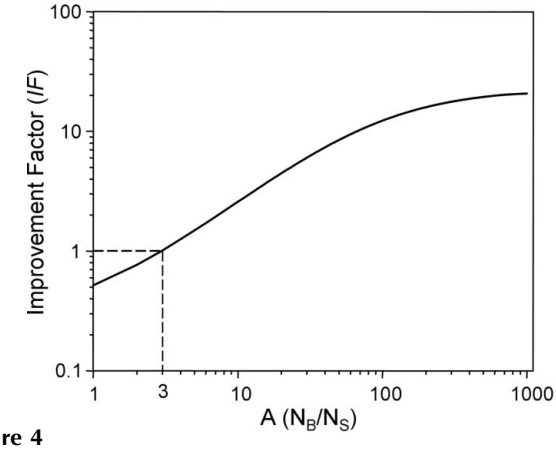

Figure 4
A log–log plot of the improvement factor (IF) *versus* $A = N_{\rm B}/N_{\rm S}$. Use of the bent crystal Laue analyzers improves the effective counts and therefore the signal-to-noise ratio.

Asymptotically, for $A \rightarrow \infty$, the improvement factor saturates at a value of $r_{\rm S}^2/r_{\rm B}$. For example, with $r_{\rm B} = 0.003$ and $r_{\rm S} = 0.26$, this approaches an improvement factor of 22.5. The background rejection in this case is somewhat favorable because of the filtering effect of the silicon, owing to the lower energy of the Fe fluorescence. This is analyzed in more detail in the following section.

4.2. Analysis for a comparison with X-ray filters

At most energies the absorption coefficient is a smooth function of energy, with a value that depends on the sample density ρ, atomic number Z, atomic mass $A_{\rm m}$ and X-ray energy E roughly as $\mu \simeq \rho Z^4/A_{\rm m} E^3$. XAFS spectra are measured by recording, directly or indirectly, the X-ray linear absorption coefficient, $\mu(E)$, as a function of energy over an absorption edge of a selected element. Between absorption edges, the absorption coefficients of all elements decrease roughly as $1/E^3$. Because of this absorption decrease, attenuators act as high-pass filters, suppressing the background while attenuating the signal to a lesser extent. For this to work effectively, the ratio between the energy of the fluorescence signal and that of the energy of the background must be sufficiently large.

If the energy of the signal and background photons are $E_{\rm S}$ and $E_{\rm B}$, respectively, and by letting $N_{\rm S} \rightarrow N_{\rm S} \exp[-\mu(E_{\rm S})\,x]$ and $N_{\rm B} \rightarrow N_{\rm B} \exp[-\mu(E_{\rm B})\,x]$, where $\mu(E_{\rm S})$ and $\mu(E_{\rm B})$ are the filter absorption coefficients at the energies of the signal and background, then the effective counts in equation (4) can be expressed as

$$N_{\rm eff} = \frac{N_{\rm S} \exp\big[-\mu\big(E_{\rm S}\big)x\big]}{1 + A\,\exp\big\{-\big[\mu(E_{\rm B}) - \mu\big(E_{\rm S}\big)\big]x\big\}}, \qquad (8)$$

where $A = N_{\rm B}/N_{\rm S}$ and $\mu(E_{\rm S})/\mu(E_{\rm B}) \cong (E_{\rm B}/E_{\rm S})^3$.

The ratio $N_{\rm eff}/N_{\rm S}$ is plotted in Fig. 5(*a*) as a function of x (filter thickness) for the case of arsenic on iron, using an aluminium attenuator to filter out the low-energy Fe fluorescence background. In this case it can be seen that an attenuator by itself is very advantageous when there is a large amount of background. The optimum thickness is a function of background-to-signal ratio A, which depends on the dilution of the system. The efficiency (effective counts/unattenuated signal counts) evaluated at the optimum attenuator thickness is plotted *versus* A in Fig. 5(*b*). The almost linear dependence indicates an approximate power law behavior as a function of A.

If the ratio $E_{\rm S}/E_{\rm B}$ is less than $\sim$1.3, however, attenuators lose their benefits altogether, and the effective counts are actually decreased if an attenuator is used. The ratio $N_{\rm eff}/N_{\rm S}$ is plotted in Fig. 6 as a function of $\mu(E_{\rm B})x$ for two different values of the energy ratio (1.5 and 2.0).

As an example, the optimum effective counts for 1% arsenic in a gallium sample are plotted *versus* A in Fig. 7. The shaded region in the plot shows optimum $N_{\rm eff}/N_{\rm S}$ for a few percent arsenic in a gallium sample. Note that in this case efficiency does not exceed 7% while the measured performance using BCLAs is 26%. This demonstrates the clear superiority of the BCLA in such cases.

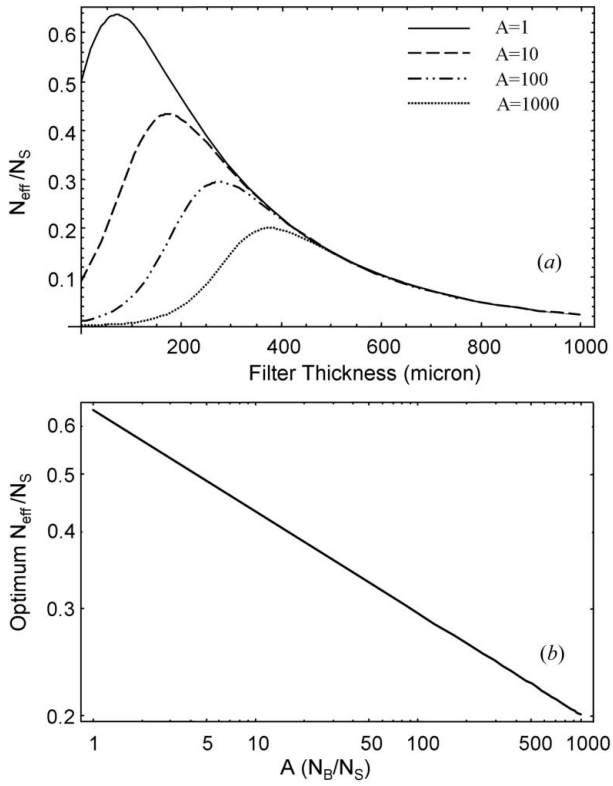

Figure 5
(*a*) The ratio $N_{\rm eff}/N_{\rm S}$ as a function of aluminium filter thickness for the case of arsenic on iron. (*b*) A log–log plot of optimum thickness *versus* background-to-signal ratio *A*.

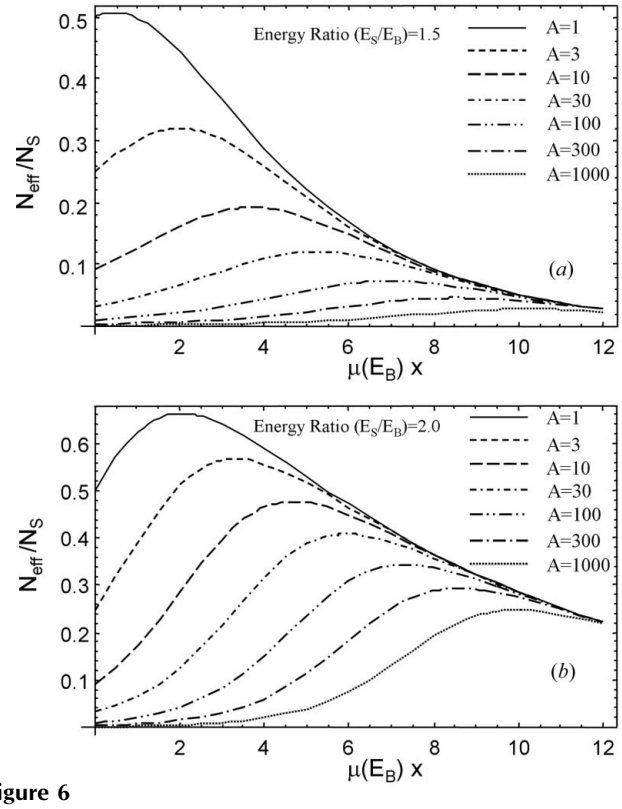

Figure 6
The ratio $N_{\rm eff}/N_{\rm S}$ as a function of filter thickness in absorption lengths of the background fluorescence energy for $E_{\rm S}/E_{\rm B}$ = 1.5 (*a*) and $E_{\rm S}/E_{\rm B}$ = 2.0 (*b*).

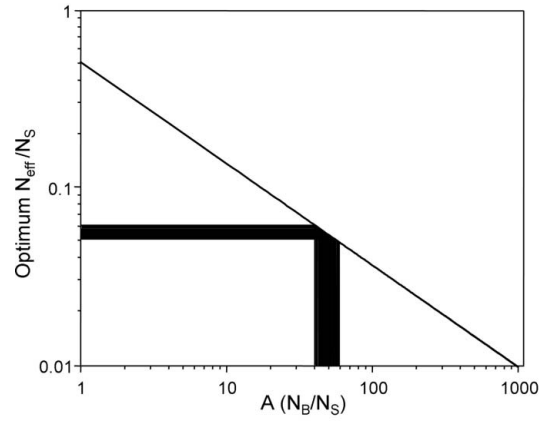

Figure 7
A log–log plot of optimum efficiency ($N_{\rm eff}/N_{\rm S}$) as a function of background-to-signal ratio *A* for 1% arsenic in a gallium sample.

5. Conclusion

Bent crystal Laue analyzers perform well and have characteristics that are both competitive with and complementary to existing detector systems. The solid angle of a single analyzer is comparable to a standard 13-element germanium detector at a distance of 10 cm. The reflection efficiency and the absorption reduce the throughput by a factor of approximately four. To achieve the same collection efficiency as a 13-element germanium detector, multi-element analyzers of the present design or units made from larger silicon wafers can be used. Multiple tiled elements are practical using a simple modular design.

BCLAs have particular advantages over filters and slits when there is an intense fluorescence background at a slightly lower energy than the fluorescence line of interest. Under such conditions X-ray filters and slits are ineffective at reducing the background, and BCLAs can serve as a very effective substitute, particularly when a focused beam is available.

Use of the Advanced Photon Source was supported by the DOE, under Contract No. W-31-109-ENG-38. GeoSoilEnviroCARS is supported by the US National Science Foundation (EAR-9906456) and US Department of Energy (DE-FG02-94ER14466). Additional support was provided by NIH-R44 RR017123-02.

References

Barrea, R. A., Gore, D., Kujala, N., Karanfil, C., Kozyrenko, S., Heurich, R., Vukonich, M., Huang, R., Paunesku, T., Woloschak, G. & Irving, T. C. (2010). *J. Synchrotron Rad.* **17**, 522–529.
Broglie, M. de & Lindemann, F. A. (1914). *CR Acad. Sci. Paris*, **158**, 944.
Bunker, G. (2010). *Introduction to XAFS: A Practical Guide to X-ray Absorption Fine Structure Spectroscopy*. Cambridge University Press.
Bunker, G. & Chapman, D. (1995). Unpublished.
Erola, E., Eteläniemi, V., Suortti, P., Pattison, P. & Thomlinson, W. (1990). *J. Appl. Cryst.* **23**, 35–42.

Etelaniemi, V., Suortti, P. & Thomlinson, W. (1989). *A Computer Program for the X-ray Reflectivity of Bent Perfect Crystals.* Report BNL-43247, National Synchrotron Light Source, Brookhaven National Laboratory, USA.
Karanfil, C., Chapman, D., Bunker, G. & Segre, C. U. (2002). *Rev. Sci. Instrum.* **73**, 1616.
Karanfil, C., Zhong, Z., Chapman, L. D., Fischetti, R., Bunker, G. B., Segre, C. U. & Bunker, B. A. (2000). *AIP Conf. Proc.* **521**, 178–182.
Kirkpatrick, P. & Baez, A. V. (1948). *J. Opt. Soc. Am.* **38**, 766–774.
Koningsberger, D. C. & Prins, R. (1988). Editors. *X-ray Absorption: Principles, Applications, Techniques of EXAFS, SEXAFS and XAFS.* New York: Wiley.
Kropf, A. J., Finch, R. J., Fortner, J. A., Aase, S., Karanfil, C., Segre, C. U., Terry, J., Bunker, G. & Chapman, L. D. (2003). *Rev. Sci. Instrum.* **74**, 4696–4702.
Kropf, A. J., Fortner, J. A., Finch, R. J., Cunnane, J. C. & Karanfil, C. (2005). *Phys. Scr.* T**115**, 998–1000.
Kujala, N. G., Karanfil, C. & Barrea, R. A. (2011). *Rev. Sci. Instrum.* **82**, 063106.
Sakayanagi, Y. (1982). *Jpn. J. Appl. Phys.* **21**, L225–L226.
Stern, E. A. & Heald, S. M. (1979). *Rev. Sci. Instrum.* **50**, 1579.
Takahashi, Y., Uruga, T., Tanida, H., Terada, Y., Nakai, S. & Shimizu, H. (2006). *Anal. Chim. Acta*, **558**, 332–336.
Zhong, Z., Chapman, L. D., Bunker, B. A., Bunker, G., Fischetti, R. & Segre, C. U. (1999). *J. Synchrotron Rad.* **6**, 212–214.